How to cite: *Angew. Chem. Int. Ed.* **2022,** *61,* e202210797
International Edition: doi.org/10.1002/anie.202210797
German Edition: doi.org/10.1002/ange.202210797

Polymerization

Perfectly Isotactic Polypropylene upon *In Situ* Activation of Ultrarigid *meso* Hafnocenes

Lucas Stieglitz[+]*, Tim M. Lenz*[+]*, Andreas Saurwein, and Bernhard Rieger**

Abstract: For more than 40 years, the synthesis of C_2-symmetric indenyl-based *racemic* metallocenes for the isoselective polymerization of propylene relied on a tedious separation of the produced *rac* and *meso* isomers. Status quo, latter are considered wasteful as they produce atactic polypropylene (aPP) rather than isotactic polypropylene (iPP) if activated with methylaluminoxane (MAO). Unexpectedly, the *in situ* activation of *meso* hafnocene **I** yielded perfectly isotactic polypropylene. We verified an isomerization of the *meso* compound to the corresponding *racemic* one upon triisobutylaluminum (TIBA) addition via nuclear magnetic resonance (NMR) spectroscopy and established an easy and convenient polymerization protocol, enabling productivities comparable to pure *rac*-**I** if applied to pure *meso*-**I** or a mixture of both isomers. With this established isomerization protocol, the potential yield of iPP was enhanced by more than 400 %. This protocol was also shown to be applicable to other *meso* hafnocenes and some initial mechanistic insights were received.

The discovery by Brintzinger and Kaminsky in 1985 producing narrow molecular weight distributed isotactic polypropylene (iPP) by employing *racemic ansa*-zirconocenes heralded a new chapter in the stereospecific polymerization of propylene besides its heterogeneous polymerization.[1] With the aid of Spaleck's pioneering preliminary work,[2] our group obtained the so far highest molecular weight and melting transition *ex reactor* of iPP by applying ultrarigid *ansa*-hafnocenes.[3] As these hafnocenes showed a poor performance at elevated temperatures, Voskoboynikov et al. investigated zirconocene-based catalysts achieving superior high-temperature performance.[4] Nevertheless, all *ansa*-metallocenes lack the same issue: the crucial and tedious separation of *rac* and *meso* isomers. This generally requires several recrystallizations,[3b] whereas for some metallocene dichlorides no suitable separation conditions have been found yet.[5] Besides this tedious and elaborative separation, a lot of valueless *meso* catalyst accumulates as a side-product and remains unused in the polymerization procedures. In literature, various *meso*-to-*rac* isomerization protocols, e.g. by applying ultraviolet (UV) light,[6] were reported to circumvent this issue—nevertheless, these protocols often led to equilibrium states or are not suitable for some catalyst systems. In 2007, Jordan et al. reported the anion-promoted *meso*-to-*rac* isomerization by applying chloride salts, such as LiCl, in refluxing tetrahydrofuran (THF).[7] This procedure has widely been examined and enforced by Voskoboynikov and co-workers for several metallocenes.[5,8] Even though the anion-promoted *meso*-to-*rac* isomerization can improve the yield of *rac* catalysts, the additional synthetic step (e.g. refluxing and removal of LiCl) and the consumed time represent serious disadvantages.

For any reason, *meso* metallocenes have not received much attention and were rather considered undesired side-products than serious pre-catalysts in the polymerization of propylene. According to Ewen's symmetry rules, *meso* catalysts are presumed to yield atactic polypropylene (aPP), as the catalyst system has no preferred direction regarding the enatiomorphic-site-model.[9] In fact, Ewen obtained an iPP/aPP blend (2:1 ratio) when polymerizing *rac/meso* Et-$(Ind)_2$–$TiCl_2$ with methylaluminoxane (MAO).[9a]

Being curious about the performance of the *meso* isomer of our group's benchmark catalyst *rac*-**I**,[4] we isolated the hafnocene *meso*-**I** (Scheme 1) and investigated its polymerization of propylene upon *in situ* activation.[10]

Instead of aPP, the polymerization employing *meso*-**I** at 30 °C yielded perfectly isotactic polypropylene if the *in situ* activation with triisobutylaluminum (TIBA) and subsequent initiation with $[Ph_3C][B(C_6F_5)_4]$ (TrBCF) was employed. Nevertheless, the productivity and molecular weight decreased for pure *meso*-**I** compared to the polymerization using pure *rac*-**I**—the polymer revealed a slight degree of bimodality (see Table 1, entries 1–4). For the polymerization using a *rac/meso* mixture, literature values were achieved with no bimodality and no reduced molecular weight.

Voskoboynikov and co-workers applied the anion-promoted *meso*-to-*rac* isomerization to *meso*-**I** to obtain *rac*-**I** with a yield of 95 %.[8] Due to the observation that *meso*-**I** yielded perfectly isotactic polypropylene ([mmmm] > 99 %)

[*] L. Stieglitz,[+] T. M. Lenz,[+] A. Saurwein, Prof. Dr. B. Rieger
Wacker-Lehrstuhl für Makromolekulare Chemie,
Catalysis Research Center,
Technische Universität München
Lichtenbergstraße 4, 85748
Garching bei München (Germany)
E-mail: rieger@tum.de

[+] These authors contributed equally to this work.

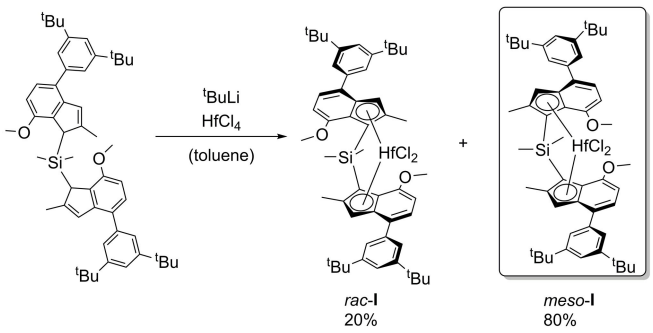

Scheme 1. Synthesis of *rac*-**I** and *meso*-**I**.

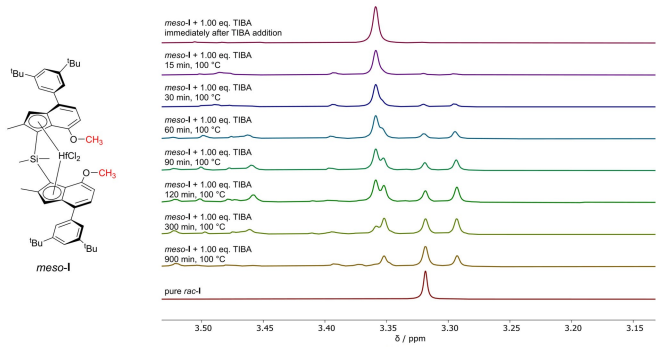

Figure 1. Excerpts of the ^{1}H NMR spectra of the isomerization of *meso*-**I** to *rac*-**I** upon addition of 1.00 equiv triisobutylaluminum (TIBA) at 100 °C.

under our polymerization conditions, we assumed that an aluminum-alkyl-induced isomerization of *meso*-**I** to *rac*-**I**—similar to the associative chloride-anion-induced one—occurs during the activation process. This was verified via nuclear magnetic resonance (NMR) analysis.

The ^{29}Si NMR of *meso*-**I** upon reaction with 20.0 equiv TIBA indicated an isomerization and subsequent alkylation of *meso*-**I** to *rac*-$\mathbf{I_{alk}}$. Herein, between several non-identifiable species, the same signal as for the activation product of *rac*-**I** with 200 equiv TIBA was observed (Figure S4). However, 200 equiv TIBA led to decomposition of *meso*-**I** and no clean NMR analysis could be conducted (Figure S5). This degradation could even be observed visually (see Figure S2), was monitored via UV/Vis analysis (Figure S1) and is probably responsible for the slight bimodality of the polymers. To investigate the isomerization in more detail, we used ^{1}H NMR analysis, initially with only 1.00 equiv TIBA to avoid signal suppression. At 60 °C, the reaction progress was rather slow, therefore, we increased the temperature to 100 °C. The isomerization was monitored via the 5*H*-indene and 4-methoxy moiety for which an increase of the *rac*-signals and a decrease of the corresponding *meso* signals (Figure 1 and S6) was observed.

Additional signals besides *rac*-signals were formed after 15 h at 100 °C, most of them can be assigned to non-identifiable degradation products. However, one signal (δ = −1.15 ppm, ^{1}H NMR) can be assigned to the alkylated *rac*-$\mathbf{I_{alk}}$ *Hf-iBu* species as it is also observable for the reaction of *rac*-**I** with 1.00 equiv TIBA under the same conditions (Figure S7). In the absence of TIBA, the ^{1}H NMR spectrum of *meso*-**I** heated to 100 °C for 15 h exhibited signals that may correspond to *rac*-**I**. However, the predominant species was still *meso*-**I**, accompanied by non-identifiable side-products, highlighting the importance of TIBA for an efficient isomerization. At 60 °C using 10.0 equiv TIBA, an isomerization of *meso*-**I** was also observed (Figure S8). As expected, the intensity of the signals corresponding to alkylated *rac*-$\mathbf{I_{alk}}$ (δ = −1.15 ppm) was increased compared to the reaction with only 1.00 equiv TIBA. However, the signals corresponding to side-products were amplified, as well. We therefore concluded that the isomerization of *meso*-**I** would concur with its degradation and that higher TIBA concentrations would promote the degradation. Furthermore, the isomerization and subsequent activation using 200 equiv TIBA was monitored via ^{29}Si NMR (Figure S9). We observed that both, *meso*-**I** and *rac*-**I** yielded the same activation product if *meso*-**I** was isomerized (1.00 equiv TIBA, 100 °C, 16 h) prior to its activation. With the isomerization using 1.00 equiv TIBA at 100 °C being more effective, we established a simple protocol for polymerizations using *meso*-**I** to yield iPP with enhanced productivity. Initially, *meso*-**I** was isomerized at 100 °C overnight—the isomerization was confirmed via NMR spectroscopy—and subsequently, the established *in situ* activation involving the pre-activation with 200 equiv TIBA was executed.[10b] This procedure yielded perfectly isotactic PP with molecular

Table 1: Conditions and results for the polymerization of propylene with hafnocene **I**.[a]

entry	catalyst	n[b]	activation[c]	[mmmm][d]	M_w[e]	T_m[f]	$Đ$[g]	P[h]
1	*meso*-**I**	1.65	TIBA/TrBCF	>99	900	165.9	2.5	500
2	*rac*-**I**	1.65	TIBA/TrBCF	>99	1600	165.1	1.6	6000
3	*rac*-**I**/*meso*-**I** (1/4)	3.30	TIBA/TrBCF	>99	1800	165.6	1.4	400
4[i]	*meso*-**I**[j]	1.65	TIBA/TrBCF	>99	700	165.0	2.4	7000
5	*rac*-**I**/*meso*-**I** (1/4) [j]	1.65	TIBA/TrBCF	>99	1300	165.0	1.6	5000
6	*meso*-**I**	3.30	MMAO	23[k]	500	163.4[k]	1.8	130

[a] t_p = 30 min; T_p = 30 °C; $V_{toluene}$ = 120 mL; $p = p_{Ar} + p_{propylene}$ = 4 bar, p_{Ar} = 1.5 bar. [b] in µmol. [c] TIBA/TrBCF: initiator $[Ph_3C][B(C_6F_5)_4]$ = 5.0 equiv, activator (TIBA) = 200 equiv, scavenger (TIBA) = 0.55 mmol; modified MAO (*MMAO*): scavenger = activator (*MMAO*) = 2000 equiv. [d] In %, determined via ^{13}C NMR spectroscopy assuming the enantiomorphic site model. [e] In kg mol^{-1}, determined absolutely via SEC-GPC in 1,2,4-trichlorobenzene at 160 °C with dn/dc = 0.097 mL g^{-1}. [f] in °C. [g] $Đ = M_w/M_n$. [h] In kg_{PP} [mol_{cat} h]$^{-1}$. [i] T_p ±15 °C. [j] Pre-isomerized with 1.00 equiv TIBA at 100 °C for 15 h. [k] aPP/iPP blend.

Table 2: Selected bond lengths and characteristic angles in the solid-state according to Rath and Coville.[13]

	bite angle [deg]	dihedral angle [deg]	Hf-$Cp_{centroid}$ [Å]	*D* [Å]
rac-**I**	57.8	42.63	2.218	0.926
meso-**I**	57.1	31.6/44.0	42.230 ± 0.003	0.927 ± 0.009
meso-$\mathbf{I_{Me}}$	56.6	32.3/44.4	2.239 ± 0.002	0.961 ± 0.004

weights, molecular weight distributions and productivities comparable to pure *rac*-**I** for a *meso/rac* mixture while the high activity and thus temperature increase for pure *meso*-**I** led to a broadened molecular weight distribution (see Table 1, entries 4 and 5).

Furthermore, we investigated the polymerization of propylene with *meso*-**I** employing MAO. The polymer obtained was a blend of iPP and aPP, chemically and physically separable (Figure S29). Unfortunately, no proper ^{1}H NMR study could be performed, as no defined catalyst species were distinguishable. We concluded that the short contact time of MAO and *meso*-**I** in the autoclave led to an incomplete isomerization of *meso*-**I** while a partial direct activation also occurred—the isomerized species yielded iPP and the directly activated one aPP. As commercial MAO always contains non-hydrolyzed trimethylaluminum (TMA),[11] the isomerization of *meso*-**I** with pure TMA at 100 °C was investigated (Figure 2).

The ^{1}H NMR spectra confirm the isomerization of *meso*-**I** upon addition of TMA, occurring even faster than with TIBA—probably due to the lower steric hindrance of TMA. In addition to *rac*-**I**, several side-products were formed if the reaction was conducted in pure toluene. However, if THF was added to the reaction mixture, neither alkylation nor degradation products were observable—only *meso*-**I** or *rac*-**I** signals. We assume that THF attenuates the reactivity of TMA, probably due to its coordinating character (Figure S10).

Nevertheless, it was still uncertain whether the isomerization is initiated by the Lewis acidity (e.g. ability to coordinate to the hafnocene) of aluminum-alkyls or upon alkylation and thus the increase of steric hindrance of the newly formed diisobutyl-moiety. Therefore, we converted *meso*-**I** with Grignard reagents according to literature known procedures.[12] While the addition of MeMgBr to *meso*-**I** yielded pure *meso*-$\mathbf{I_{Me}}$, the reaction of *meso*-**I** or *rac*-**I** with *i*BuMgBr did not yield the desired *meso*-$\mathbf{I_{iBu}}$ or *rac*-$\mathbf{I_{iBu}}$, even if performed under various reaction conditions.

Compared to *meso*-**I**, single crystal X-ray diffraction (SC-XRD) revealed for *meso*-$\mathbf{I_{Me}}$ an increased C–Si–C angle, Hf–$Cp_{centroid}$ bond-length and *D*-value due to the enhanced bulkiness by the methyl groups, leading to a reduced bite angle (Table 2, Figure 3). Furthermore, *meso*-**I** and *meso*-$\mathbf{I_{Me}}$ feature two configurations of the 4(3,5*t*Bu)-aryl substituents, probably due to the steric repulsion of the indenyl substituents. This explains the lack of a perfect symmetry of *meso* isomers, leading to a variation in Hf–$Cp_{centroid}$ and the dihedral angle, that was also observed for the respective *meso* zirconocene in a previous study.[3a] Nevertheless, the isolation of *meso*-$\mathbf{I_{Me}}$ illustrates that the steric repulsion arising from the activation is not responsible for the isomerization and that Grignard reagents lack the ability to isomerize *meso*-**I**.

The polymerization using *rac/meso* mixtures employing the *in situ* activation with TIBA/TrBCF enables a fast and convenient screening for the performance of ultrarigid hafnocenes, as no tedious separation is required and comparable molecular weights as for pure *rac* isomers are obtained. Furthermore, by using the established isomerization protocol, the potential yield of iPP per utilized ligand for the catalyst-synthesis is enhanced by a multiple (more than 400 % for **I**).

Up to now we cannot conclude whether the isomerization is caused by effects of the substituents inside the catalyst framework—especially the methoxy moiety—influencing the coordination of aluminum-alkyls. Nevertheless, the 4(3,5*R*)-aryl substituents were proven to not play a crucial role, as an isomeric *rac/meso* mixture (1/3) of a 4-Ph-indene hafnocene[3b] yielded perfectly isotactic PP as well. So far, we were not yet able to isolate the pure *meso* isomer but

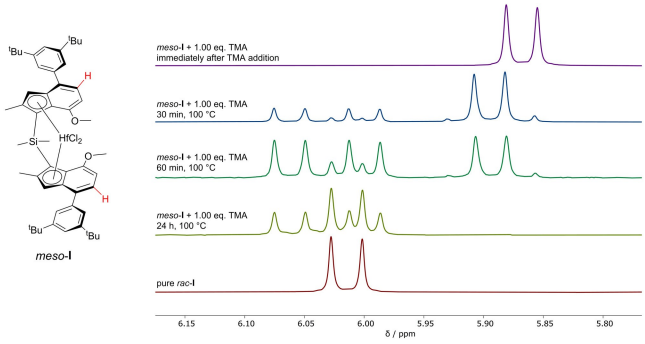

Figure 2. Excerpts of the ^{1}H NMR spectra of the isomerization of *meso*-**I** to *rac*-**I** upon addition of 1.00 equiv trimethylaluminum (TMA) at 100 °C.

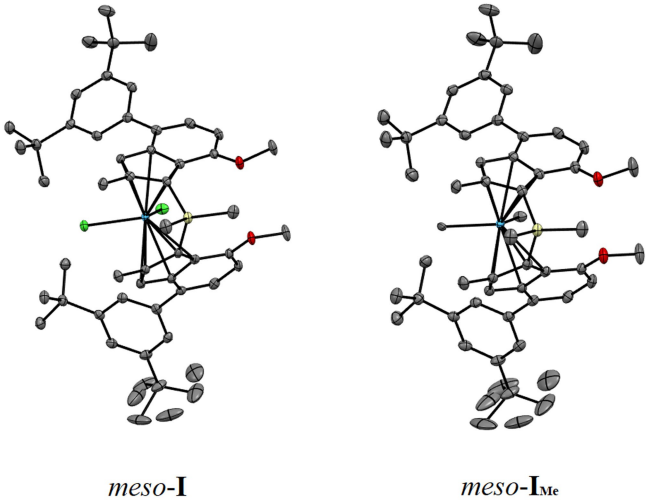

Figure 3. ORTEP style representation of *meso*-**I** and *meso*-$\mathbf{I_{Me}}$ with ellipsoids drawn at 50 % probability level. Hydrogen atoms omitted for clarity.

no signals corresponding to the respective *meso* isomer were visible in the ^{1}H NMR spectrum after the mixture was isomerized according to our protocol. Additionally, the catalyst's productivity in propylene polymerization was enhanced for the isomerized mixture compared to the non-isomerized one.

In summary, we proved the isomerization of *meso*-**I** to *rac*-**I** with aluminum-alkyl species, yielding perfectly isotactic polypropylene with macromolecular characteristics equivalent to that of pure *rac*-**I** if activated *in situ.* Furthermore, the established isomerization protocol prior to *in situ* activation led to a productivity of pure *meso*-**I** comparable to pure *rac*-**I**, also adaptable for isomeric mixtures. Finally, via the synthesis of *meso*-$\mathbf{I_{Me}}$ we excluded the steric hindrance in the course of the activation to initiate the isomerization, as pure *meso*-$\mathbf{I_{Me}}$ was isolated without any trace of isomerization, both in solution and as single crystals. To further prove our hypothesized associative mechanism, additional catalyst systems with differing ligand frameworks and central metal atoms have to be examined and density functional theory (DFT) calculations have to be performed in the future.

Acknowledgements

The authors thank Dr. Sergei Vagin for constructive discussions and Jonas Bruckmoser, Moritz Kränzlein and Dr. Thomas Pehl for proofreading the manuscript and for valuable discussions. Furthermore, we thank Fabrizio Napoli from the Prof. Roland Fischer research group for the LIFDI mass spectra. Open Access funding enabled and organized by Projekt DEAL.

Conflict of Interest

The authors declare no conflict of interest.

Data Availability Statement

SC-XRD data is available from https://www.ccdc.cam.ac.uk/products/csd with deposition numbers 2179591 (*meso*-**I**) and 2179592 (*meso*-$\mathbf{I_{Me}}$).[13]

Keywords: Activation · Hafnocenes · Isomerization · Isotactic Polypropylene · Metallocenes

[1] W. Kaminsky, K. Külper, H. H. Brintzinger, F. R. W. P. Wild, *Angew. Chem. Int. Ed. Engl.* **1985**, *24*, 507–508; *Angew. Chem.* **1985**, *97*, 507–508.

[2] a) W. Spaleck, M. Antberg, J. Rohrmann, A. Winter, B. Bachmann, P. Kiprof, J. Behm, W. A. Herrmann, *Angew. Chem. Int. Ed. Engl.* **1992**, *31*, 1347–1350; *Angew. Chem.* **1992**, *104*, 1373–1376; b) W. Spaleck, F. Kueber, A. Winter, J. Rohrmann, B. Bachmann, M. Antberg, V. Dolle, E. F. Paulus, *Organometallics* **1994**, *13*, 954–963.

[3] a) A. Schöbel, E. Herdtweck, M. Parkinson, B. Rieger, *Chem. Eur. J.* **2012**, *18*, 4174–4178; b) M. R. Machat, D. Lanzinger, A. Pöthig, B. Rieger, *Organometallics* **2017**, *36*, 399–408.

[4] a) G. P. Goryunov, M. I. Sharikov, A. N. Iashin, J. A. M. Canich, S. J. Mattler, J. R. Hagadorn, D. V. Uborsky, A. Z. Voskoboynikov, *ACS Catal.* **2021**, *11*, 8079–8086; b) V. V. Izmer, A. Y. Lebedev, D. S. Kononovich, I. S. Borisov, P. S. Kulyabin, G. P. Goryunov, D. V. Uborsky, J. A. M. Canich, A. Z. Voskoboynikov, *Organometallics* **2019**, *38*, 4645–4657; c) P. S. Kulyabin, G. P. Goryunov, M. I. Sharikov, V. V. Izmer, A. Vittoria, P. H. M. Budzelaar, V. Busico, A. Z. Voskoboynikov, C. Ehm, R. Cipullo, D. V. Uborsky, *J. Am. Chem. Soc.* **2021**, *143*, 7641–7647.

[5] P. S. Kulyabin, V. V. Izmer, G. P. Goryunov, M. I. Sharikov, D. S. Kononovich, D. V. Uborsky, J. A. M. Canich, A. Z. Voskoboynikov, *Dalton Trans.* **2021**, *50*, 6170–6180.

[6] a) A. L. Rheingold, N. Robinson, J. Whelan, B. Bosnich, *Organometallics* **1992**, *11*, 1869–1876; b) W. Kaminsky, A.-M. Schauwienold, F. Freidanck, *J. Mol. Catal. A* **1996**, *112*, 37–42; c) F. R. Wild, L. Zsolnai, G. Huttner, H. H. Brintzinger, *J. Organomet. Chem.* **1982**, *232*, 233–247.

[7] R. M. Buck, N. Vinayavekhin, R. F. Jordan, *J. Am. Chem. Soc.* **2007**, *129*, 3468–3469.

[8] A. Vittoria, G. P. Goryunov, V. V. Izmer, D. S. Kononovich, O. V. Samsonov, F. Zaccaria, G. Urciuoli, P. H. Budzelaar, V. Busico, A. Z. Voskoboynikov, *Polymer* **2021**, *13*, 2621.

[9] a) J. A. Ewen, *J. Am. Chem. Soc.* **1984**, *106*, 6355–6364; b) H. H. Brintzinger, D. Fischer, R. Mülhaupt, B. Rieger, R. M. Waymouth, *Angew. Chem. Int. Ed. Engl.* **1995**, *34*, 1143–1170; *Angew. Chem.* **1995**, *107*, 1255–1283; c) L. Resconi, L. Cavallo, A. Fait, F. Piemontesi, *Chem. Rev.* **2000**, *100*, 1253–1346.

[10] a) M. Schloegl, C. Troll, U. Thewalt, B. Rieger, *Z. Naturforsch. B* **2003**, *58*, 533–538; b) L. Stieglitz, D. Henschel, T. Pehl, B. Rieger, *Organometallics* **2021**, *40*, 4055–4065.

[11] V. Busico, R. Cipullo, R. Pellecchia, G. Talarico, A. Razavi, *Macromolecules* **2009**, *42*, 1789–1791.

[12] M. R. Machat, A. Fischer, D. Schmitz, M. Vöst, M. Drees, C. Jandl, A. Pöthig, N. P. M. Casati, W. Scherer, B. Rieger, *Organometallics* **2018**, *37*, 2690–2705.

[13] a) P. C. Möhring, N. J. Coville, *Coord. Chem. Rev.* **2006**, *250*, 18–35; b) R. M. Shaltout, J. Y. Corey, N. P. Rath, *J. Organomet. Chem.* **1995**, *503*, 205–212, Deposition Numbers 2179591 (for *meso*-**I**) and 2179592 (for *meso*-$\mathbf{I_{Me}}$) contain the supplementary crystallographic data for this paper. These data are provided free of charge by the joint Cambridge Crystallographic Data Centre and Fachinformationszentrum Karlsruhe Access Structures service.

Manuscript received: July 22, 2022
Accepted manuscript online: September 20, 2022
Version of record online: October 17, 2022